Technical Memorandum

To: Kim Schofield

From: Lauren Gardner, Gonzalo Rada, Gary Elkins, Kevin Senn and Nick Weitzel

cc: Mustafa Mohamedali

Date: July 31, 2020 (original); May 21, 2021 (revised)

Re. Forensic Desktop Study Report: Texas LTPP Test Section 48_1096

The Long-Term Pavement Performance GPS 1 Asphalt Concrete (AC) on Granular Base test section 48_1096[1] was nominated for a desktop study under TPF-5(332) "LTPP Forensic Evaluations." Since placement of an AC overlay in 2001, the test section has shown a steady increase in wheel path cracking, while at the same time maintaining an acceptable level of pavement roughness. Additionally, aggressive crack sealing has been applied to the test section, which does not appear to have been properly captured in the LTPP database. Therefore, this test section is being investigated in order to: (1) examine the rapid rise in wheel path/fatigue related cracking after the 2001 overlay, (2) provide a history of crack sealing performed on the test section in order to update the contents of the LTPP database, and (3) perform a comparison between pavement design models predictions and observed pavement performance.

SITE DESCRIPTION

LTPP test section 48_1096 is located on U.S. 90, westbound, in Medina County, Texas. U.S. 90 is a rural principal arterial with two lanes in the direction of traffic. It is classified as being in a Wet, No-Freeze climate zone with an average annual precipitation ranging between 14 inches (2011) and 52 inches (2007). The test section has an annual average air freezing index ranging between 0 deg-F deg-days (multiple years) and 47 deg-F deg-days (1989) during the performance period in question. The coordinates (in degrees) of the test section are 29.3559, -98.83502. Photograph 1 shows the test section at Station 0+00 looking westbound in 2017, while Map 1 shows the geographical location of the test section relative to San Antonio, Texas.

[1] First two digits in test section number represent the State Code [48 = Texas]. The final four digits are unique within each State/Province and were assigned at the time the test section was accepted into the LTPP program.

Wood Environment & Infrastructure Solutions, Inc.
12000 Indian Creek Ct, Suite F
Beltsville, MD 20705
+1 301-210-5105
www.woodplc.com

Photograph 1. LTPP Section 48_1096 at Station 0+00 looking westbound in 2017.

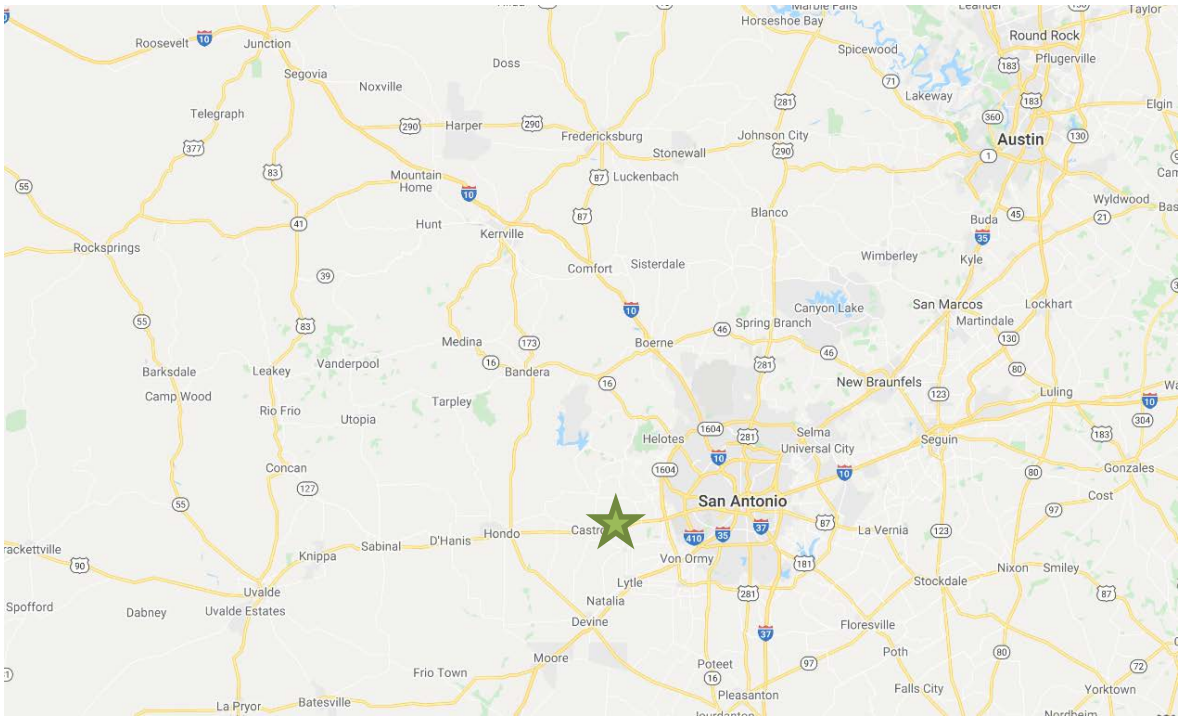

Map 1. Geographical location of test section relative to San Antonio, Texas.

BASELINE PAVEMENT HISTORY

This section of the document presents historical data on the pavement structure and its structural capacity, climate, traffic, and pavement distresses.

Pavement Structure and Construction History

Test section 48_1096 was constructed in 1981 and incorporated in the LTPP program in 1987 as a GPS-1 site. The original pavement structure for the test section at the time of its incorporation into the LTPP program is summarized in Table 1; this information corresponds to CONSTRUCTION_NO = 1 (CN = 1) in the LTPP database. The next construction event occurred in 1996 when a 0.3-inch aggregate seal coat (chip seal) was applied to the test section (CN=2) as summarized in Table 2. On May 30, 2001, the test section received an additional 0.3-inch aggregate seal coat (chip seal). Two weeks later (June 15, 2001), the test section received a 2-inch AC overlay and became a part of the GPS-6B AC Overlay with Conventional Asphalt Cement on AC Pavement, No Milling experiment. These two construction events were combined and considered collectively as CN=3. The pavement structure of CN=3 is depicted in Table 3.

Table 1. Pavement structure for CN =1

Layer Number	Layer Type	Thickness (in.)	Material Code Description
1	Subgrade (untreated)		Fine-Grained Soils: Fat Clay with Sand
2	Bound (treated) subbase	6.0	Lime-Treated Soil
3	Unbound (granular) base	8.1	Crushed Stone
4	Asphalt concrete layer	0.0	Fog Seal
5, 6 and 7	Asphalt concrete layer	7.1	Hot Mixed, Hot Laid AC, Dense Graded

Table 2. Pavement structure for CN =2

Layer Number	Layer Type	Thickness (in.)	Material Code Description
1	Subgrade (untreated)		Fine-Grained Soils: Fat Clay with Sand
2	Bound (treated) subbase	6.0	Lime-Treated Soil
3	Unbound (granular) base	8.1	Crushed Stone
4	Asphalt concrete layer	0.0	Fog Seal
5, 6 and 7	Asphalt concrete layer	7.1	Hot Mixed, Hot Laid AC, Dense Graded
8	Asphalt concrete layer	0.3	Chip Seal

Table 3. Pavement structure for CN =3

Layer Number	Layer Type	Thickness (in.)	Material Code Description
1	Subgrade (untreated)		Fine-Grained Soils: Fat Clay with Sand
2	Bound (treated) subbase	6.0	Lime-Treated Soil
3	Unbound (granular) base	8.1	Crushed Stone
4	Asphalt concrete layer	0.0	Fog Seal
5, 6 ad 7	Asphalt concrete layer	7.1	Hot Mixed, Hot Laid AC, Dense Graded
8 and 9	Asphalt concrete layer	0.6	Chip Seals
10	Asphalt concrete layer	2.0	Hot Mixed, Hot Laid AC, Dense Graded

While the construction events described above are the only events called out in the LTPP pavement history dataset, pictures of the test section over time and the amount of sealed cracking reported in the manual distress surveys indicate crack sealing was applied to the section prior to the March 1995, November 2013, and January 2017 distress surveys. The application of crack sealing during these periods does not have a significant effect on the structural capacity of the pavement, but these maintenance events are important to note as sealed cracks are recorded and included in the total count of cracks observed on the test section over time. Moreover, they can affect the performance of the pavement by preventing water from reaching the subsurface layers, and especially the unbound layers. Further discussion of the crack sealing applied at this site is included in the section on the pavement distress history.

Pavement Structural Properties

Figure 1 shows the average Falling Weight Deflectometer (FWD) deflection under the nominal 9,000-pound load plate over time. The deflection of the sensor located in the center of the load plate is a general indication of the total "strength" or response of all layers in the pavement structure to a vertically applied load. This deflection can be influenced by pavement temperature at the time of testing, precipitation, and moisture to name a few of the main factors. As depicted in Figure 1, the deflections observed on the site fluctuate over time. The reported deflections at the load plate are highest in June 1996 (17.4 mils) and August 2000 (17.9 mils), which correspond to high temperature (86°F) collection dates as depicted in Table 4. The next highest temperature (84°F) collection date occurred in August 2003, but the deflection observed was significantly lower (11.2 mils); however, this is likely the direct result of the 2.3 inch AC overlay applied in June 2001, which provided increased structural capacity. Overall, the measured deflections ranged between 8.4 and 17.9 mils from 1990 to 2017.

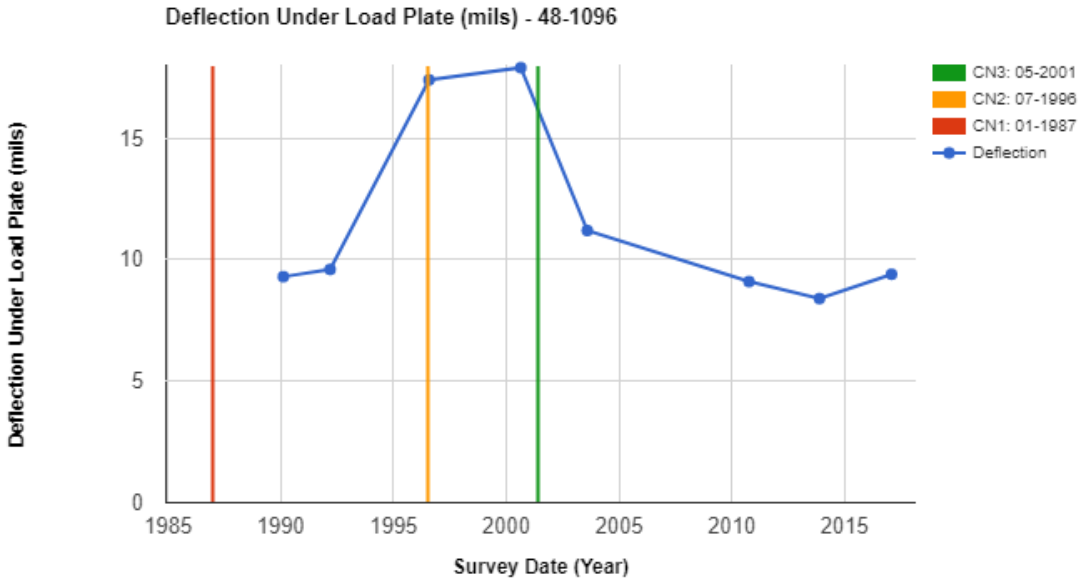

Figure 1. Time history of average deflection for the sensor located in the load plate normalized to 9,000 lb. drop load.

Table 4. Average air temperature during deflection testing.

Date	Mean daily air temperature (from MERRA) the week leading up to the test date (deg F)
2/12/1990	61
3/11/1992	58
7/29/1996	86
8/23/2000	86
8/5/2003	84
10/6/2010	68
11/20/2013	62
1/30/2017	51

The layer moduli backcalculated from the deflection data were also assessed for the test section. Prior to the overlay in 2001, the pavement structure was modeled as a 7.1-inch AC layer (Layer 1) over 8.1 inches of typical granular base (Layer 2), 30 inches of fine subgrade, and a semi-infinite subgrade layer (Layer 4). Following the overlay, the pavement structure was modeled as a 9.1-inch AC layer (Layer 1) over 8.1 inches of typical granular base (Layer 2), 30 inches of fine subgrade, and a semi-infinite subgrade layer (Layer 4). The backcalculated moduli for each layer are shown in Figures 2 through 5 for six of the eight FWD testing dates – February 1990, March 1992, July 1996, August 2000, August 2003, and October 2010. Backcalculated layer moduli were not calculated for November 2013 and January 2017, and therefore, not included in the LTPP database.

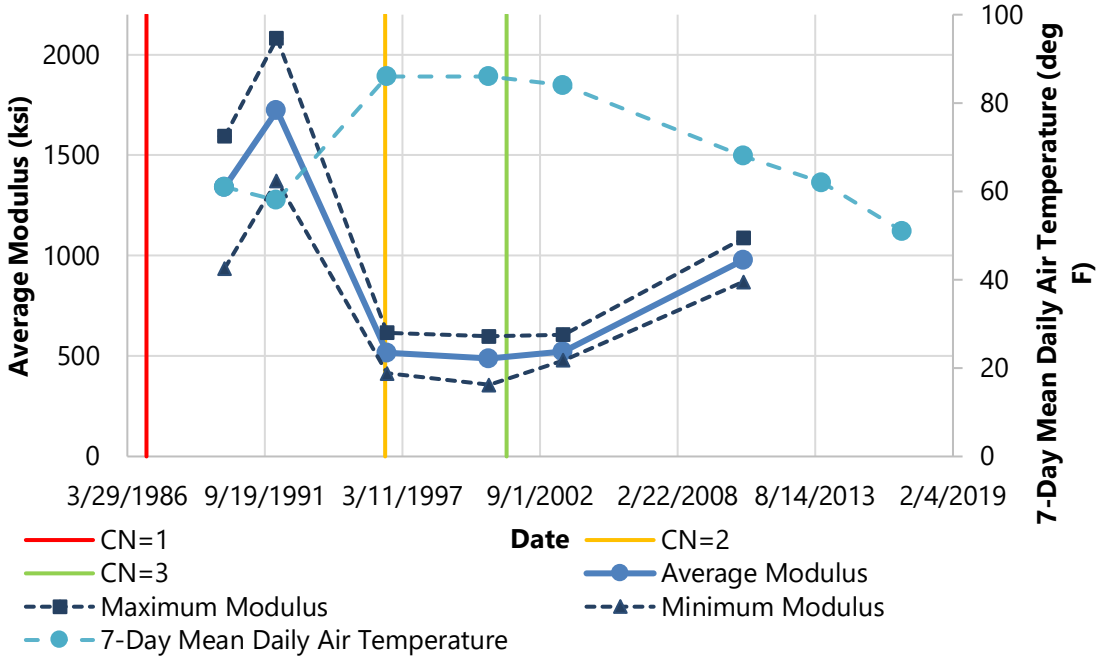

Figure 2. Average backcalculated modulus for AC layer (Layer 1).

Figure 2 shows the backcalculated AC layer moduli as well as the 7-day mean daily air temperature. As shown, the values range between 490 and 1,750 ksi, which appears to be quite reasonable. Moreover, there is a clear relationship between AC layer modulus and temperature – as the temperature goes up the modulus go down and vice-versa. The three lowest AC moduli (between 490 and 530 ksi) were backcalculated for the three test dates with the highest temperatures (between 84 and 86°F). Similarly, the two highest AC layer moduli (1,750 and 1,340 ksi) correspond to the two testing dates with the lowest temperatures (58 and 61°F).

Figure 3 shows the backcalculated unbound granular base layer moduli as well as the cumulative precipitation on the seven days leading up to the test date (based on VWS data). As shown, layer moduli range between 8 and 63 ksi, which like the backcalculated AC layer moduli, appear quite reasonable. This is especially true when viewed in light of precipitation – in general, as precipitation decreases the backcalculated granular base layer moduli increases. For example, the highest moduli values (39, 45 and 63 ksi) occur when the 7-day cumulative precipitation is zero. The exceptions are in 1992 when a much lower moduli value would have been anticipated given the amount of precipitation and in 1996 when despite a low precipitation value the moduli did not substantially increase. Nonetheless, the results generally appear to be reasonable.

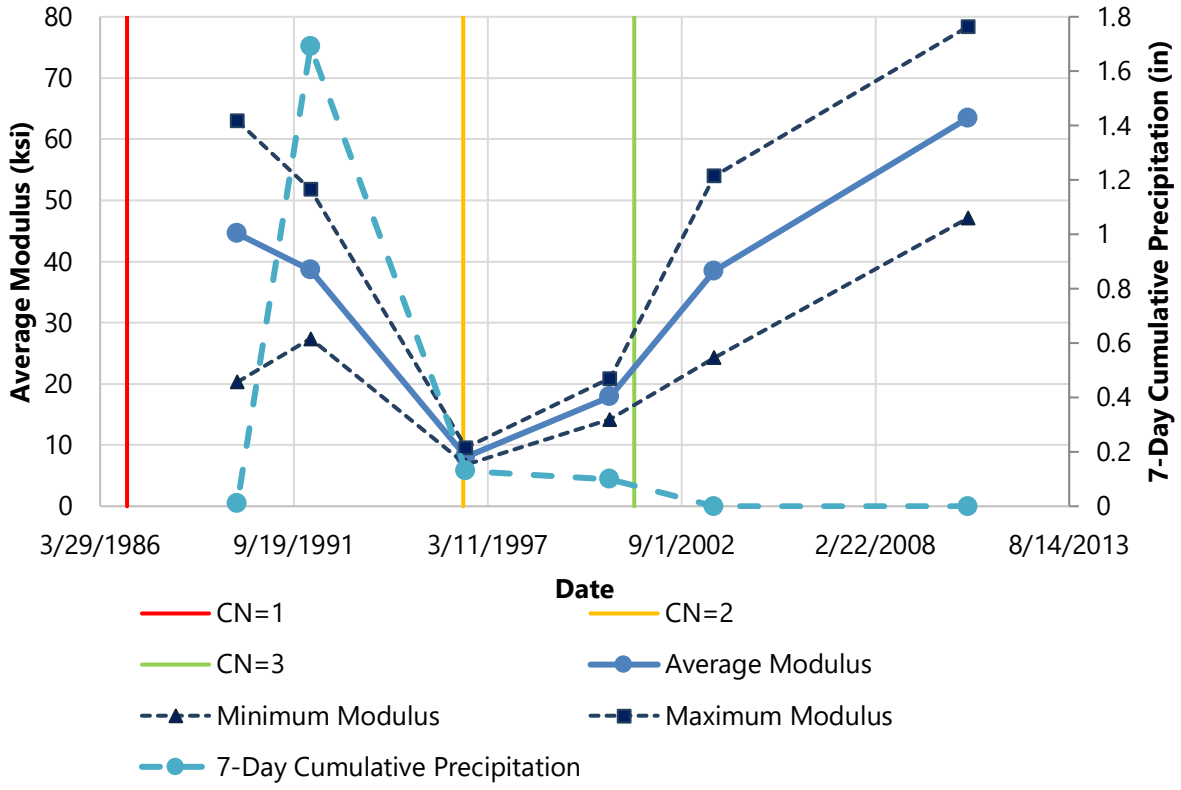

Figure 3. Average backcalculated modulus for granular base (Layer 2).

Figures 4 and 5 show the backcalculated layer moduli for the top 30 inches of subgrade and for the subgrade below those 30 inches (assumed semi-infinite), respectively, as well as the cumulative precipitation on the seven days leading up to the test date (based on VWS data). For both layers the moduli vary over a small and reasonable range – about 11 to 15 ksi and 20 to 25 ksi, respectively. The most significant deviation occurs on the July 1996 testing date, when the modulus of the top 30 inches of

subgrade drastically increases to 48 ksi, while the value for the subgrade layer beneath significantly drops to 15 ksi. It is strongly suspected that this is the result of compensating layer moduli effects; i.e., during backcalculation one modulus value for one layer went up so the value of the other layer had to go down. The results also appear to indicate that the two subgrade layer moduli are not as sensitive to precipitation as was the case with the unbound granular base layer.

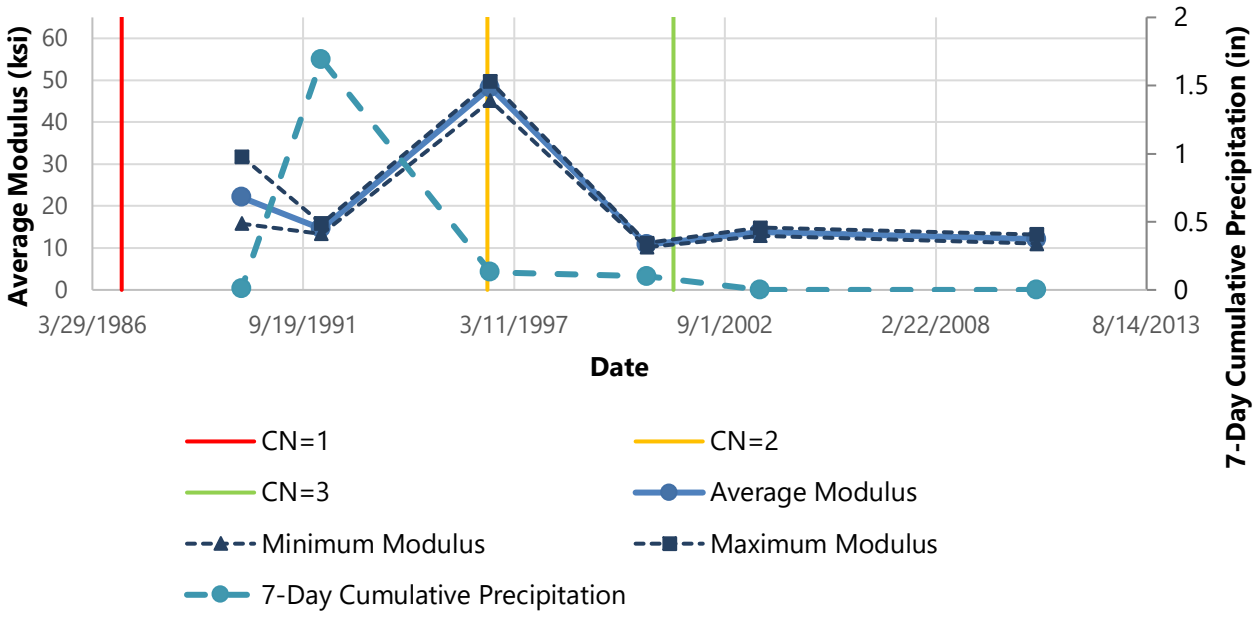

Figure 4. Average backcalculated modulus for fine subgrade (Layer 3).

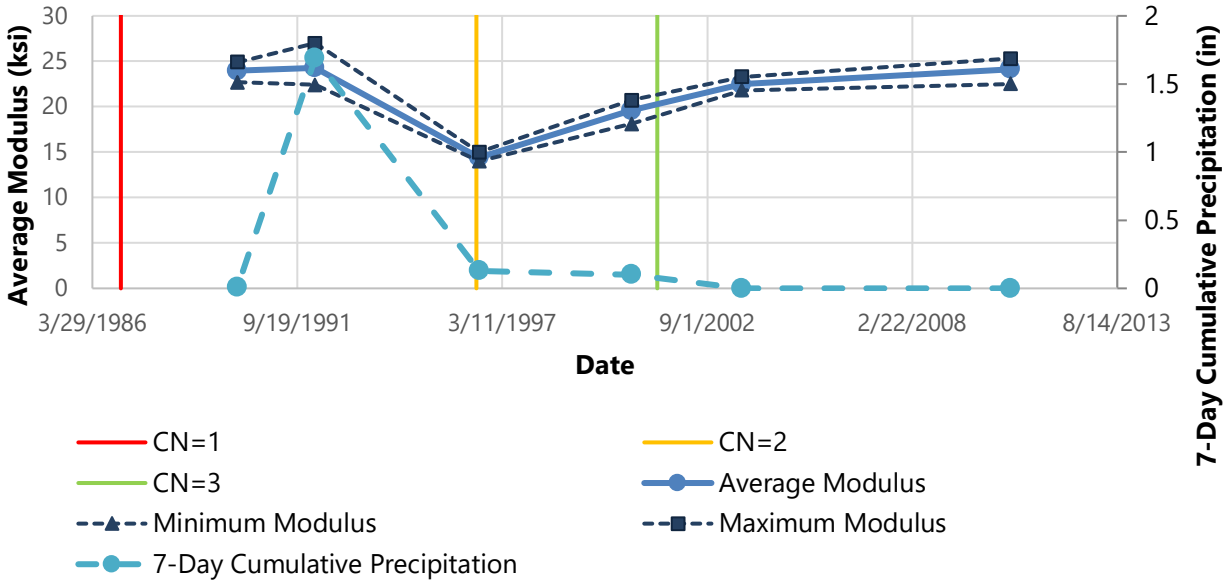

Figure 5. Average backcalculated modulus for semi-infinite subgrade (Layer 4).

In summary, the backcalculated layer moduli appear reasonable for all four layers. Moreover, some of the variations in the layer moduli values may be explained in terms of compensating layer moduli effects, as indicated earlier for the subgrade layers. Another potential cause for the variations is the difference in the number of basins included in averaging the drop load and deflection basins. Because the same test section is being assessed, the number of basins used should be consistent throughout time. However, the average number of basins used for February 1990, March 1992, July 1996, August 2000, August 2003, October 2010, and November 2013 was 55, 84, 52, 74, 81, and 83, respectively. The low number of basins used in the backcalculations for 1990 and 1996 also correspond to the greatest Root Mean Square Errors (RMSE), indicating the lack of basins used to backcalculate the moduli affected the goodness of fit of the backcalculations.

The above conclusion about the reasonableness of the backcalculated layer moduli is further confirmed by comparing the results to those derived from laboratory resilient modulus testing. Table 5 summarizes the laboratory test results. For the AC layer, moduli values are shown for three test temperatures – 41, 77 and 104°F, respectively. For the unbound granular base and subgrade layers, various statistical results are provided for the range of stress states (confining and deviatoric stresses) to which the laboratory sample were subjected.

Table 5. Laboratory Resilient Modulus Test Results

Layer	Temperature (°F)	Number of Samples/test results	Range of moduli values (ksi)	Range of Confining Stress (psi)	Range of Maximum Nominal Axial Stress (psi)
AC	41	1 sample (2 test results)	2,365-2,458	N/A	N/A
	77	1 sample (2 test results)	958-986	N/A	N/A
	104	1 sample (2 test results)	421-425	N/A	N/A
Base	N/A	2 samples (15 test results each)	12.8 to 81.2 (Average of 37.1)	3 to 20	3 to 40
Subgrade	N/A	2 samples (15 test results each)	5.1 to 13.2 (Average of 9.3)	2 to 6	2 to 10

As shown in Figure 6, the AC modulus versus temperature relationship for the field- and lab-derived resilient modulus is excellent – i.e., the trend defined by the two datasets appears to be very reasonable. Similarly, the field- versus lab-derived resilient moduli for the granular base and subgrade layers moduli also appear to agree well. For the granular base layer, the field-derived values range between 8 and 63 ksi, while those from the lab range between 13 and 81 ksi. In the case of the subgrade layer, the field-derived values range between 10 and 50 ksi versus 5 to 13 ksi from the laboratory testing. A more precise comparison of the layer moduli for the unbound granular layers was considered beyond the scope of this study and hence it was not pursued. Such comparison would require (1) the computation of the universal resilient modulus equation coefficients (K1, K2 and K3) based on lab measured moduli at various stress states, (2) the estimation of the stress states for the pavement structure in question and assumed load(s) (e.g., 9,000 lbs), and (3) the computation of the representative modulus of the granular base and subgrade layers.

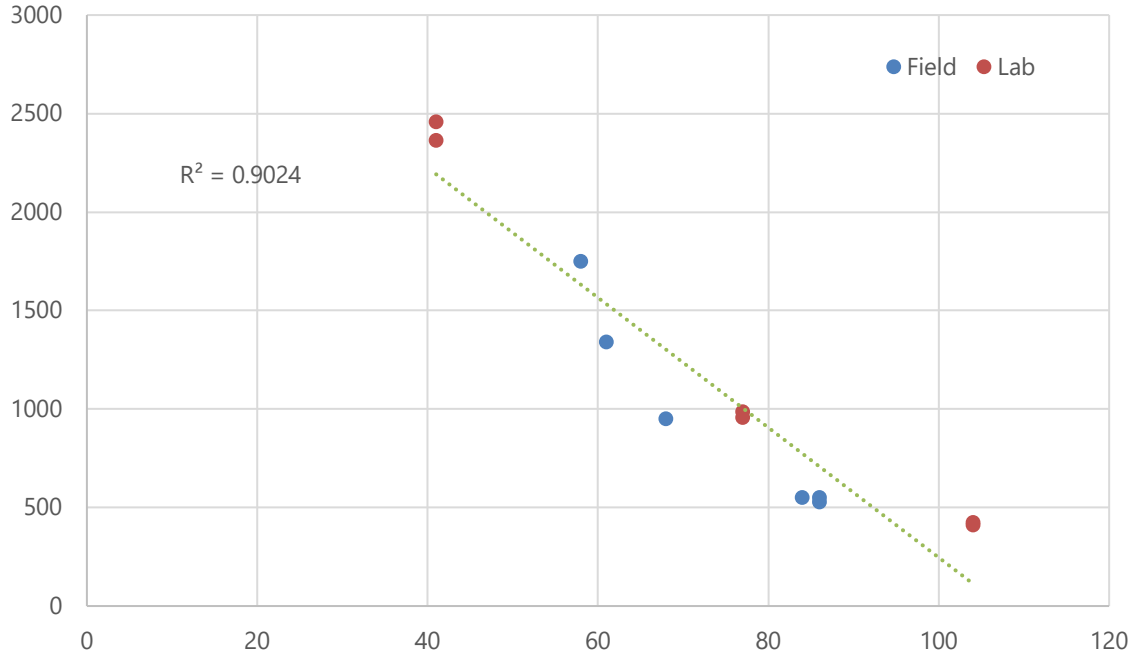

Figure 6. Field- and lab-derived AC resilient modulus values.

Assessment of Pavement Design Model Predictions Using Lab and Field Results

One of the objectives of this desktop study was to compare pavement design model predictions and observed pavement performance. To accomplish this, the AASHTO 1972 Interim Guide modified flexible pavement empirical design equation was used to assess the pavement performance using both lab and field data – it was assumed that this guide was used in the design of the original pavement test section. The equation for estimating the number of 18-kip ESALs that the pavement section can be subjected to over its useful life is:

$$logW_{18} = 9.36 * \log(SN + 1) - 0.20 + \frac{\log\left[\frac{4.2-p_t}{4.2-1.5}\right]}{0.40+\frac{1094}{(SN+1)^{5.19}}} + log\frac{1}{R} + 0.372(S_i - 3.0) \quad [2]$$

where:

W_{18} : Number of 18-kip equivalent single axle loads (ESALs)
SN: Structural number (the sum of the product of the thickness and the corresponding layer coefficient for the surface, base, and subbase layers)
p_t: Terminal serviceability at end of design life
R: Regional support factor
S_i: Soil support value

[2] AASHTO (1972). *AASHTO Interim Guide for Design of Pavement Structures*, American Association of State Highway and Transportation Officials, Washington, D.C.

For the pavement test section in question, p_t was assumed to be 2.5 and R was assumed to be 1.25 (test section location fell between 1 and 1.5 based on a map of the regional support factors in accordance with NCHRP Report 128).[3] It is recommended that these assumptions be confirmed through coring and interviews with TxDOT staff in the follow-up investigation to this desktop memorandum.

The test section was next modeled as 7.1 inches of AC, 8.1 inches of granular base, and subgrade with lab-derived layer moduli of 1,317 ksi, 36 ksi, and 10 ksi and field-derived layer moduli of 948, 27 and 22 ksi, respectively. The lab-derived moduli of the base and subgrade layers were assumed to be the median resilient moduli for the layers based on sample testing under different confining pressures and axial stressed (TST_UG07_SS07_WKSHT_SUM), while the field-derived values the back calculated moduli for each layer were averaged for the period between CN=1 and CN=2. The lab-derived AC modulus was assumed to be the average, temperature-adjusted resilient modulus for the AC overlay in 2001 (Layer 10). While the focus of this analysis is on the pavement structure prior to 2001, because data on the AC resilient moduli for 1990 was limited, the modulus of the 2001 AC overlay was assumed for the AC layer prior to CN=3. The field-derived AC modulus was also assumed to be the average temperature-corrected moduli.

A third analysis was conducted with field data adjusted using backcalculation correction factors.[4] The backcalculation correction factors, which were first introduced in the *Mechanistic-Empirical Pavement Design Guide—A Manual of Practice*, are utilized to improve the harmonization between field-derived resilient modulus values and laboratory-derived resilient modulus values for the aggregate base and subgrade layers. The correction factors were utilized to convert the backcalculated resilient moduli to equivalent laboratory values. The estimated moduli for the field-derived moduli in this study therefore decreased to 17 ksi and 7.7 ksi for the granular base and subgrade layers after being multiplied by a correction factor of 0.62 and 0.35, respectively. Subsequently, these reduced moduli values resulted in a decrease in estimated the SN and S_i used to calculated W_{18}. All other values used in the field-derived calculations remained the same.

Based on the inputs detailed above, which are summarized in Table 6, the number of W_{18} was calculated to be 94.5 million, 311.6 million, and 17.2 million for the lab-,field-, and corrected field-derived datasets, respectively. The high W_{18} value calculated for the field-derived data is a result of a high modulus value (22 ksi) reported for the subgrade; subsequently, the high subgrade value resulted in a higher-than-expected S_i estimation which appears to have led to an overestimation of W_{18}. When compared to the actual traffic values reported on the test section, which are presented later in this technical memorandum, it appears that the pavement structure was over-designed based on as-constructed conditions or, more likely, that the anticipated truck traffic was over-estimated. When considering the corrected field-derived datasets, the design of the pavement structure seems more appropriate based on traffic observed on the section.

[3] Van Til, C. J. , McCullough, B. F. , Vallerga, B. A. , and Hicks, R. G. (1972). *NCHRP Report 128: Evaluation of AASHO Interim Guides for Design of Pavement Structures*. HRB, National Research Council, Washington, D.C.
[4] AASHTO. (2015). Mechanistic-Empirical Pavement Design Guide - A Manual of Practice. Washington, DC: American Association of State Highway Transportation Officials.

Table 6. Pavement design variables

Variable		Lab-derived Values	Field-derived Values	Corrected Field-derived Values
SN	$a_{1\ (AC)}$	0.56	0.55	0.55
	$d_{1\ (AC)}$	7.1 in	7.1 in	7.1 in
	$a_{2\ (gran.\ base)}$	0.16	0.13	0.08
	$d_{2\ (gran.\ base)}$	8.1 in	8.1 in	8.1 in
	SN	5.272	4.958	4.553
p_t		2.5	2.5	2.5
R		1.25	1.25	1.25
S_i		6.3	8.2	5.5
W_{18}		94.5 million	311.6 million	17.2 million

Climate History

The time history for average annual precipitation (from MERRA) since 1981 is shown in Figure 7. In 2007, the amount of precipitation appears to be a local high (52 inches), while the low (14 inches) was recorded in 2011. The mean precipitation recorded at the site is 28 inches for the period shown in Figure 7; in general, less precipitation was reported following 2007. While there are high amounts of precipitation reported on this section, no specific annual precipitation events are notable. Instead, the high amounts of precipitation reported near the test section is likely a result of recurrent storms that occur in this area. In addition to the reported precipitation, it was also noted there is an irrigation system adjacent to the test section, which may also lead to increased moisture at the site.

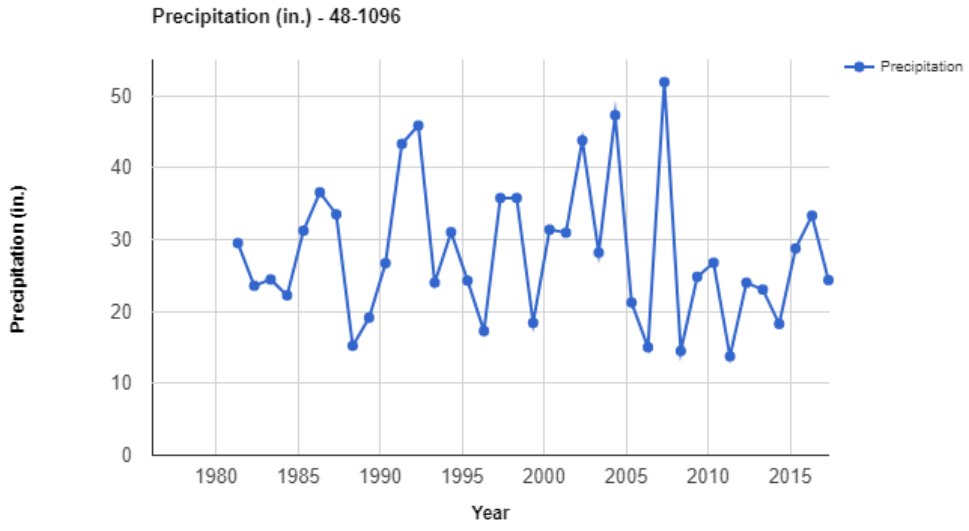

Figure 7. Average yearly precipitation over time.

Figure 8 shows the time history of the average annual freezing index (from the MERRA) for the test site. The freezing index is the summation of the difference between freezing temperature and the average air temperature when it is less than freezing over a year's time. This index is an indicator of the harshness of

the winter season relative to issues such as ground frost and low temperature cracking in pavements. As depicted in Figure 8, the freezing index values ranged from 0 (multiple years) to 47 (in 1989)—which is well below the 150 deg F deg days used to classify a freeze region—indicating it is not a likely factor negatively affecting test section performance.

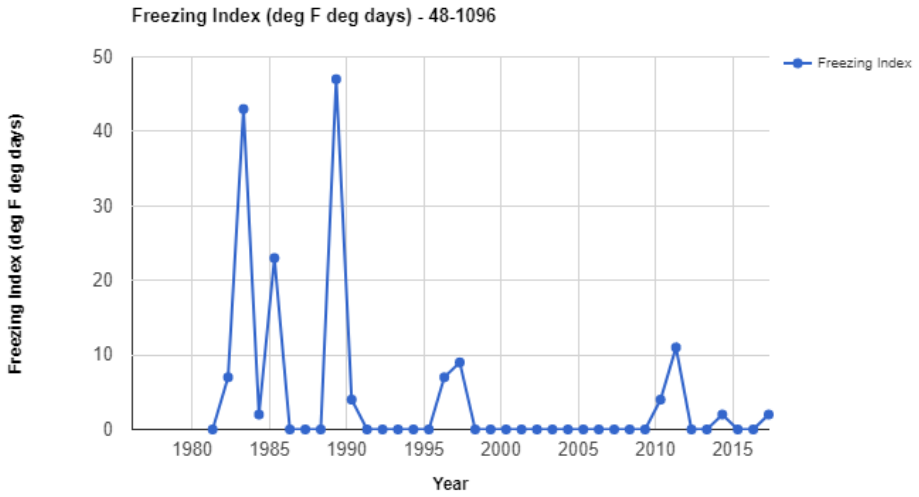

Figure 8. Average annual freezing index over time.

Truck Volume History

Figure 9 shows the annual average daily truck traffic (AADTT) data in the LTPP test lane by year. The annual truck traffic counts increase from 203 in 1981 to 1,181 in 2017, or approximately 27 additional trucks per year. While there is a consistent increase in truck traffic along this section, a spike in truck traffic is observed in between 2008 and 2012. This spike may be related to unrealistic monitored class data which are used to calculate the AADTT during that period. The average number of ESALs reported on this section also increased over time. The number of ESALS increased from 44,250 in 1981 to 362,095 in 2017, or approximately 8,829 ESALs per year as depicted in Figure 10. The figure also depicts the number of cumulative ESALs over time. At the time of the overlay in 2001, a cumulative 3,044,910 ESALs were reported. By 2017, a cumulative 7,820,348 ESALs were reported—further confirming the pavement structure as constructed was overdesigned.

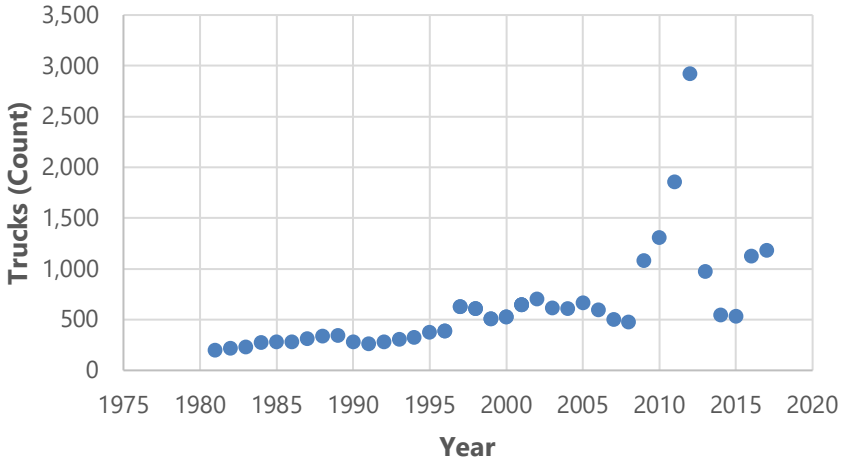

Figure 9. Average annual daily truck traffic (AADTT) history.

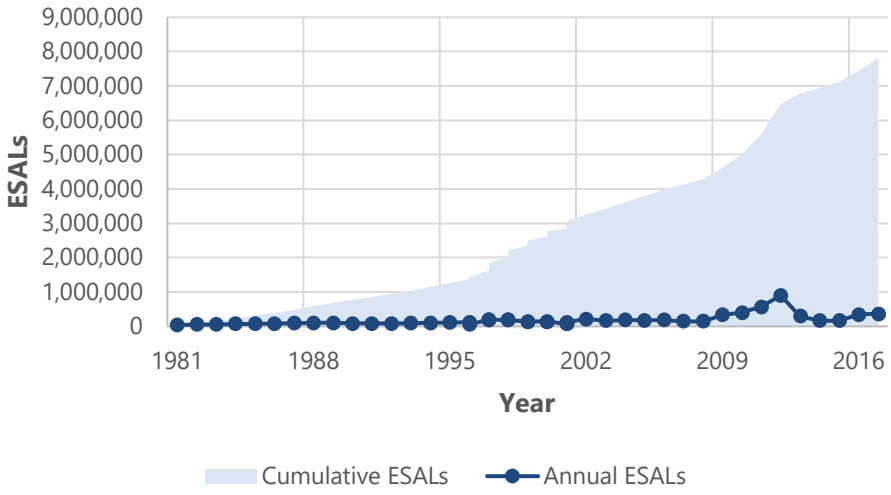

Figure 10. Estimated annual and cumulative ESAL for vehicle classes 4-13 over time.

Pavement Distress History

The following section summarizes the distresses observed on the test section between the time the section was constructed and 2017, which is when the last manual distress survey was performed on the test section. Fatigue/alligator cracking, longitudinal cracking (inside and outside the wheel path), transverse cracking, IRI, and rutting were assessed. No block cracking or patching was observed.

Fatigue/Alligator Cracking

Figure 11 shows the total area of fatigue related cracking observed on the section. As the fatigue cracking observed on the section is limited to the wheel paths, it is hypothesized that it is the result of bottom-up cracking. Prior to the AC overlay in 2001, bottom-up cracking is not observed until 1999 when 4 ft^2 was reported on the section. Following the overlay in 2001, the area of the test section where fatigue cracking was observed increased over time. Fatigue cracking was first observed on the section in 2006, 5 years after the AC overlay, when 111 ft^2 of fatigue cracking was observed. Once the cracking had initiated, it propagated at an average rate of 20 ft^2/year between 2006 and 2017. By 2017, 336 ft^2 of fatigue cracking was observed.

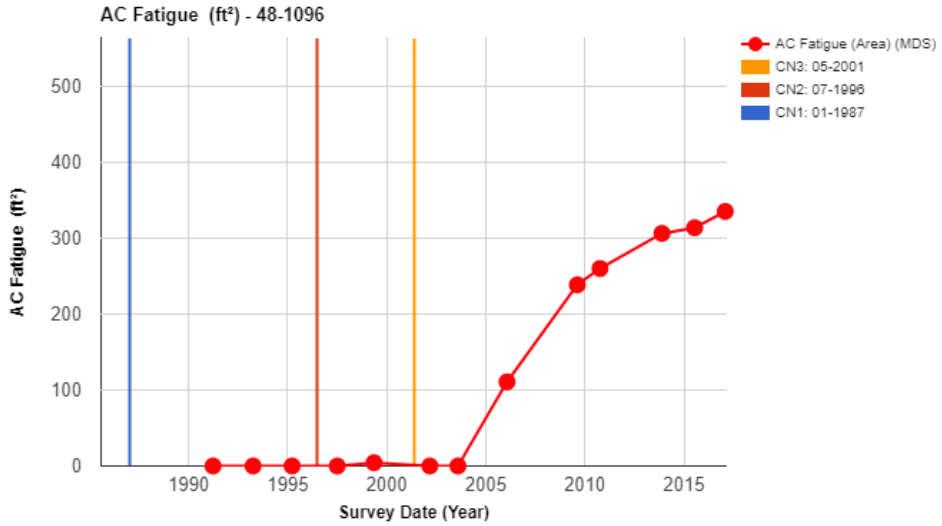

Figure 11. Time history of the area of bottom-up cracking.

The increase observed in bottom-up cracking following the AC overlay may be the result of increased precipitation and traffic in the early to mid-2000s. As water infiltrates the pavement layers, the base and subgrade tend to weaken (especially when reaching saturation conditions) causing the increase in fatigue cracking observed. Similarly, the increase in traffic loadings over time may have also contributed to the fatigue cracking of the AC surface layer. Finally, the increase in cracking observed between 2006 and 2017 may be the result of aging (and more appropriately oxidizing) of the AC surface layer, leading to a more brittle material prone to fatigue cracking.

Longitudinal Cracking

Data on longitudinal cracking, inside and outside the wheel path, was collected between 1991 and 2017 as shown in Figures 12 and 13. In 1993, 32 total feet of non-wheel path (NWP) longitudinal cracking was reported, 12 years after the construction of the test section. By 1995, the NWP longitudinal cracking increased to 435 feet, at a rate of 202 feet/year between 1993 and 1995. Following the chip seal in 1996 (CN=2), the NWP longitudinal cracking observed on the section dropped to zero. NWP longitudinal cracking was not observed again until 1999, three years after the application of the aggregate seal coat when 12 feet of NWP longitudinal cracking was observed. After the application of the AC overlay in 2001, NWP longitudinal cracking was not reported again until 2009, 8 years after CN=3, when 23 feet of NWP longitudinal cracking was observed. Once cracking was initiated, it propagated at a rate of 8 feet/year between 2009 and 2017. NWP longitudinal cracking was predominantly observed near the lane edge.

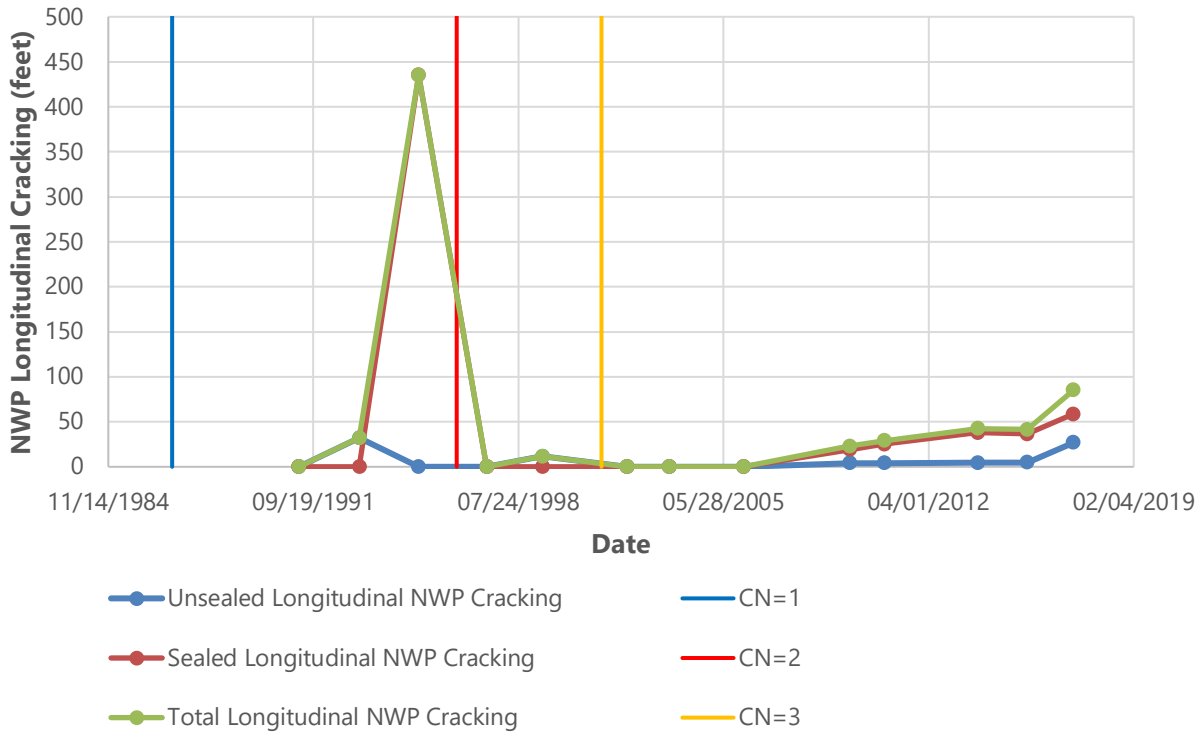

Figure 12. Time history of the length of NWP longitudinal cracks.

The spike in NWP longitudinal cracking observed in 1995 appears to be related to the crack sealing applied to the section between 1993 and 1995. As depicted in Figure 14, while there are very few visible cracks on the pavement section in 1993, the section is heavily crack sealed by 1995. This indicates that between these two distress surveys, the test section received aggressive crack sealing that is not indicated in the LTPP pavement history. Based on the limited cracking observed in 1993, it is assumed the crack

sealing applied during this time included areas of pavement that did not have cracking. Therefore, the spike in cracking during this period is related to an increase in sealed "cracks" rather than a spike in cracking as depicted in Figure 12.

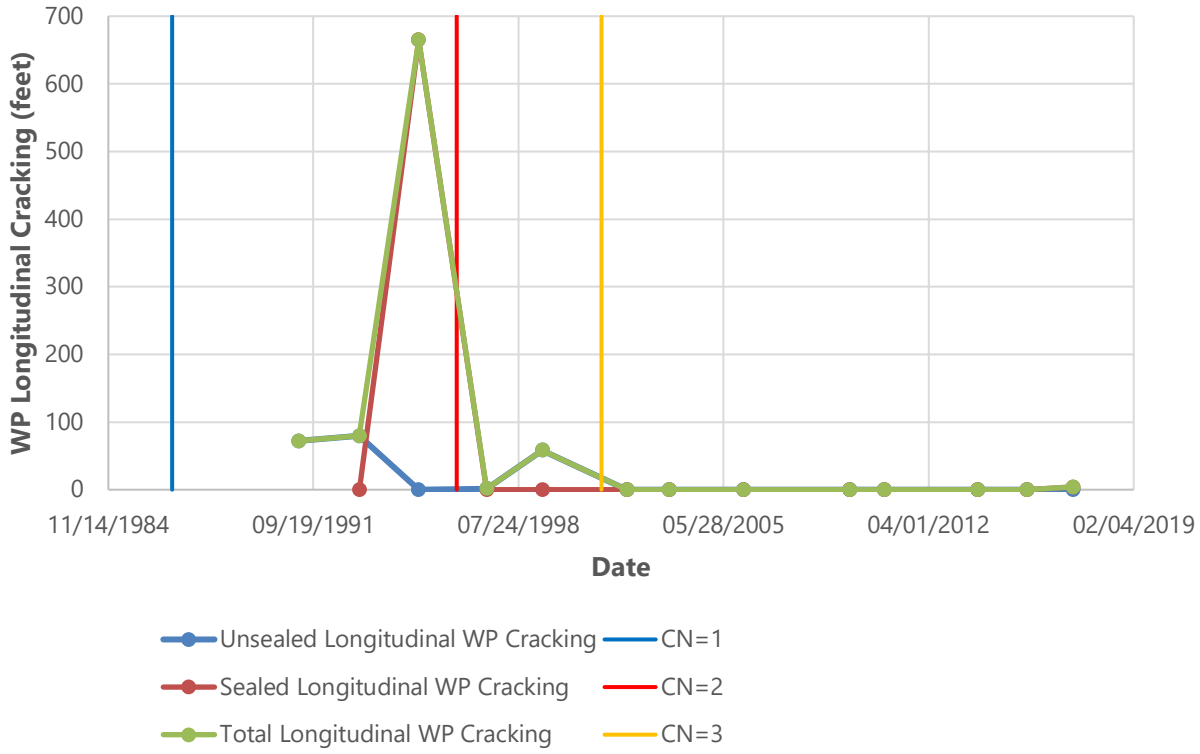

Figure 13. Time history of the length of WP longitudinal cracks.

Figure 14. Test section at Station 5+00 looking westbound in 1993 (left) and 1995 (right) depicting an increase in crack sealing during this period.

Longitudinal cracking inside the wheel path (WP) appears along the section during the first reported manual distress survey in 1991, when 72 total feet of longitudinal WP cracking was reported. The amount

of WP longitudinal cracking continues to increase prior to the aggregate seal coat in 1996 (CN=2). Prior to the application of the chip seal, 665 feet of WP longitudinal cracking is observed on the section in 1995. Like NWP longitudinal cracking, the spike in WP longitudinal cracking reported in 1995 is likely the result of aggressive crack sealing applied between 1993 and 1995 as depicted in Figure 13. Based on the limited cracking observed in 1993, it is assumed the crack sealing applied during this time included areas of pavement that did not have cracking. Therefore, the spike in cracking during this period is related to an increase in sealed "cracks" rather than a spike in cracking. Following CN=2 in 1996, the WP longitudinal cracking observed on the section dropped to nearly zero (1.3 feet observed in 1997). Notable WP longitudinal cracking was not observed again until 1999, 3 years after the application of the chip seal, when 58 feet of WP longitudinal cracking was observed. After the application of the AC overlay in 2001, WP longitudinal cracking was not reported again until 2017, 16 years after CN=3, when 4 feet of WP longitudinal cracking was observed. In summary, other than the 1995 spike, limited WP and NWP longitudinal cracking has occurred on the test section.

Transverse Cracking

Data on transverse cracking was collected between 1991 and 2017 as shown in Figures 15 and 16. Transverse cracking was first reported in 1993, 12 years after the construction of the test section, when 8 feet (3 cracks) of cracking was reported. The transverse cracking spiked in 1995 when 127 feet (35 cracks) of cracking was observed. Like longitudinal cracking, the spike in transverse cracking reported in 1995 is likely the result of aggressive crack sealing applied between 1993 and 1995. Based on the limited cracking observed in 1993, it is assumed the crack sealing applied during this time included areas of pavement that did not have cracking. Therefore, the spike in cracking during this period is related to an increase in sealed "cracks" rather than a spike in cracking.

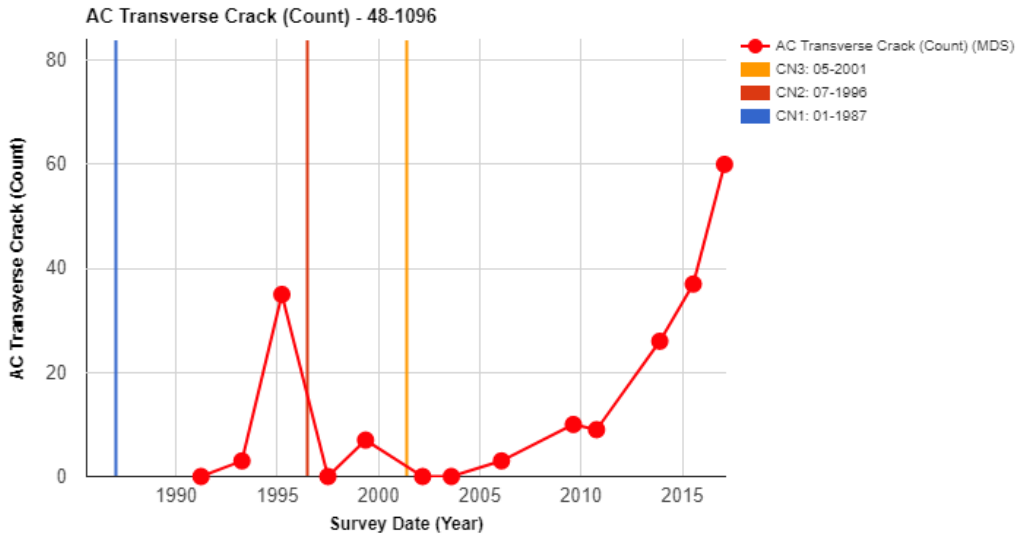

Figure 15. Time history of the number of transverse cracks.

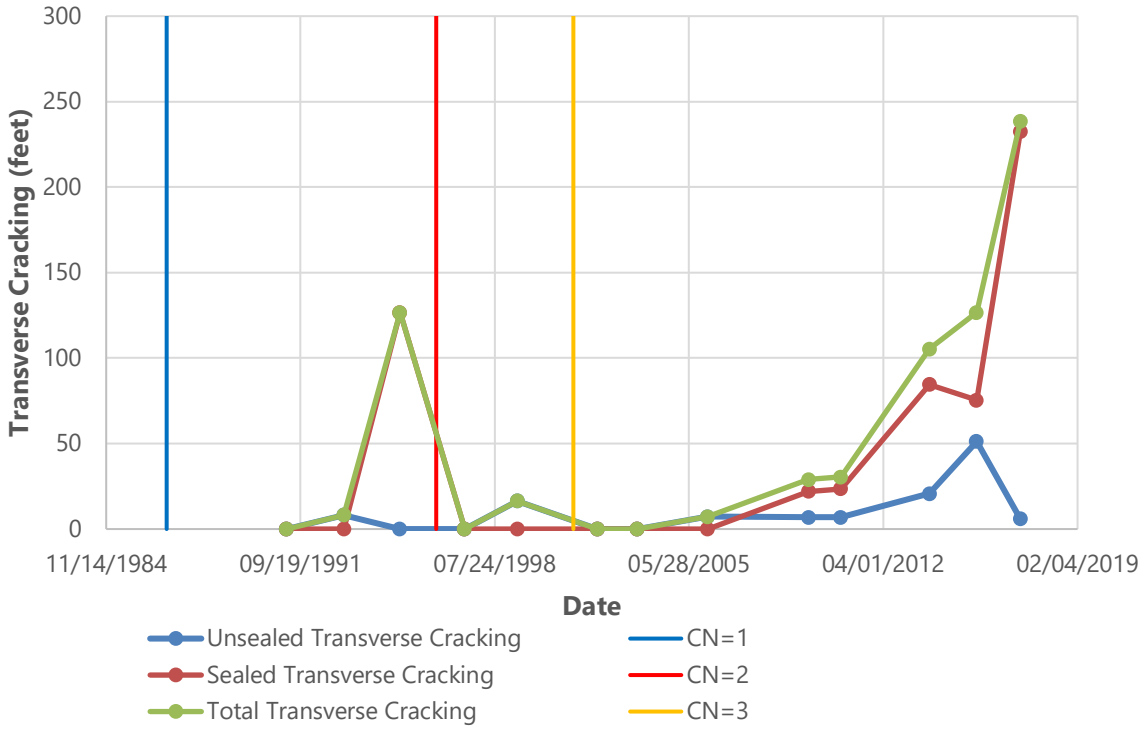

Figure 16. Time history of the length of transverse cracking.

Following CN=2 in 1996, no transverse cracking is observed again until 1999 when 16 feet (7 cracks) was observed. The transverse cracking observed drops to zero following the AC overlay in 2001. It is not until 2006, 5 years after CN=3, that 7 feet of transverse cracking (3 cracks) is reported. Once the cracking initiated, it propagated at a rate of 21 feet/year between 2006 and 2017. In 2017, 239 feet of transverse cracking was reported, which is the equivalent of a full transverse crack every 20 ft along the length of the test section.

The spike in transverse cracking observed in 2017 may be related to the crack sealing applied to the section between 2015 and 2017. While there was some transverse cracking observed in 2015, the section appears more heavily crack sealed by 2017. This indicates that between these two distress surveys, the test section received additional crack sealing, which is not indicated in the LTPP pavement history. The crack sealing applied during this time may have included areas of pavement that did not have cracking. The increase observed in transverse cracking may also be the result of increased precipitation in the early to mid-2000s as well as pavement aging.

IRI

The average IRI measurements for the test section over time are shown in Figure 17. Prior to the AC overlay in 2001, the IRI reported on the test section increased from 135 in/mile in 1990 to 165 in/mi in 1998, at a rate of 3.75 in/mile/year. The pavement's IRI performance was classified as "Fair" based on FHWA performance definitions. Following the AC overlay in 2001, the IRI on the section dropped to 66 in/mile in 2002. The IRI reported subsequently increased to 95 in/mile in 2016, increasing at a rate of 2 in/mile over 14 years. The pavement's IRI performance was classified as "Good" during this period based on FHWA performance definitions.

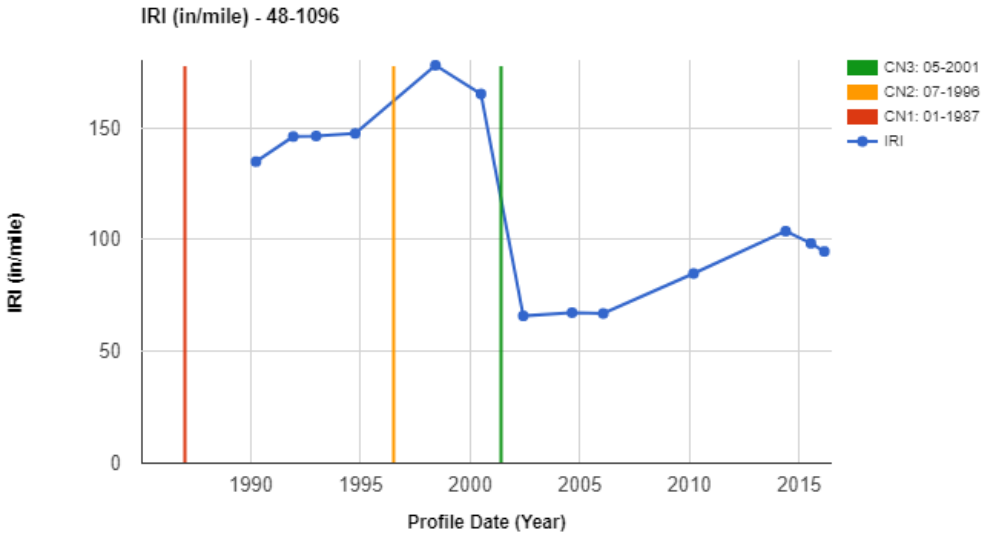

Figure 17. Time history plot of pavement roughness.

Rutting

The rutting observed over time on the test section is shown in Figure 18. Prior to the overlay in 2001, the rut depths observed fluctuated, with an average reported rut depth of 0.36 inches. Following the overlay in 2001, the rutting observed on the section decreased to 0.16 inches in 2002. The rutting increased slightly between 2002 and 2017 reaching a rut depth of 0.28 inches in 2017.

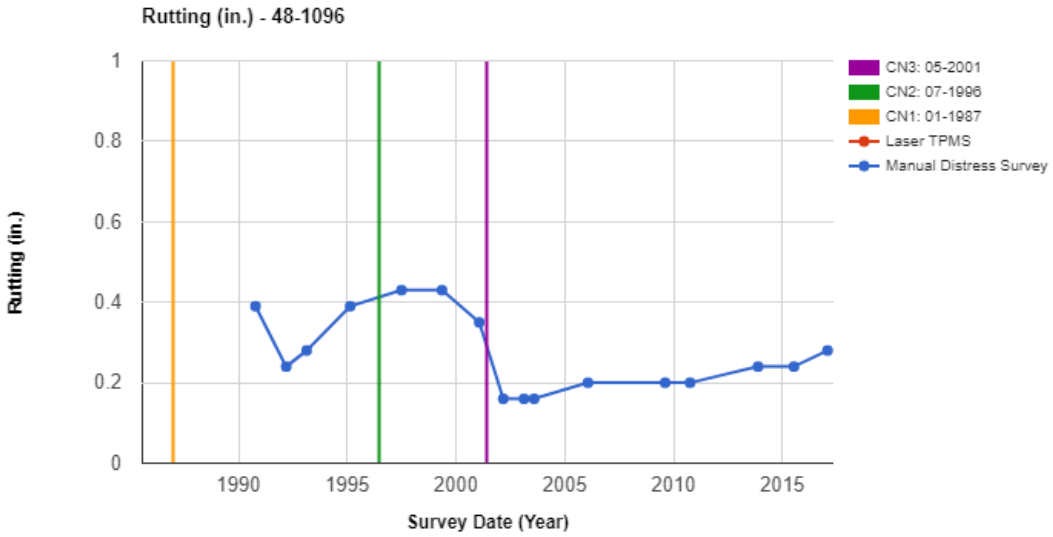

Figure 18. Time history plot of average rut depth computations.

In addition to the average rut depth observed over time, the change in the transverse profile of the test section prior to the 2001 overlay was also investigated. Using the transverse profiles of the test section, an analysis of the predominant layer the plastic deformation occurs was assessed using the method

developed in NCHRP 01-34a.[5] The method, which was derived using finite element analyses of rutting mechanisms in the HMA surface, base, and subgrade, is focused on the transverse profile characteristics indicative of permanent deformation such as densification, shear failure, or shear flow.

The methodology consists of two key steps: calculation of distortion parameters and the use of criteria to classify the lowest layer in the pavement structure contributing to the ruts. Distortion parameters include the maximum rut depth (D), positive area, and negative area of a transverse profile. For each profile, the wire method is used to assess the maximum rut depth, which is the greatest perpendicular distance measured from the pavement surface to the wire reference line as depicted in Figure 19. Similarly, the positive area (A_P) and negative area (A_N) are the sum of the areas above and below the transverse profile reference line, respectively. Using these parameters, the ratio of positive area to negative area (R), total area (A_T), and the theoretical total areas for the HMA, base, and subgrade failure (C_1,C_2, and C_3, respectively) are calculated and used to assess the failed layer. The assessment of the parameters used to determine the lowest layer contributing to the pavement's surface deformation is described in Figure 20.

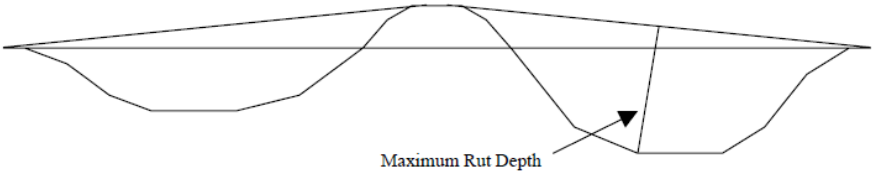

Figure A-1. Definition of maximum rut depth.

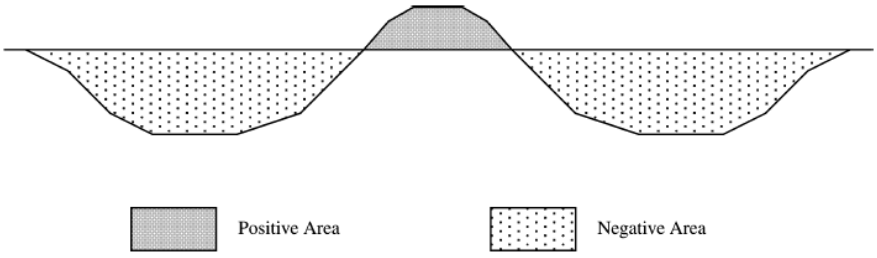

Figure 19. Transverse profile maximum rut depth and positive and negative areas (White et al., 2002)

[5] White, T., J. Haddock, A.J.T. Hand, & H. Fang. NCHRP 468: *Contributions of Pavement Structural Layers to Rutting of Hot Mix Asphalt Pavements*. National Cooperative Highway Program, Washington D.C., 2002.

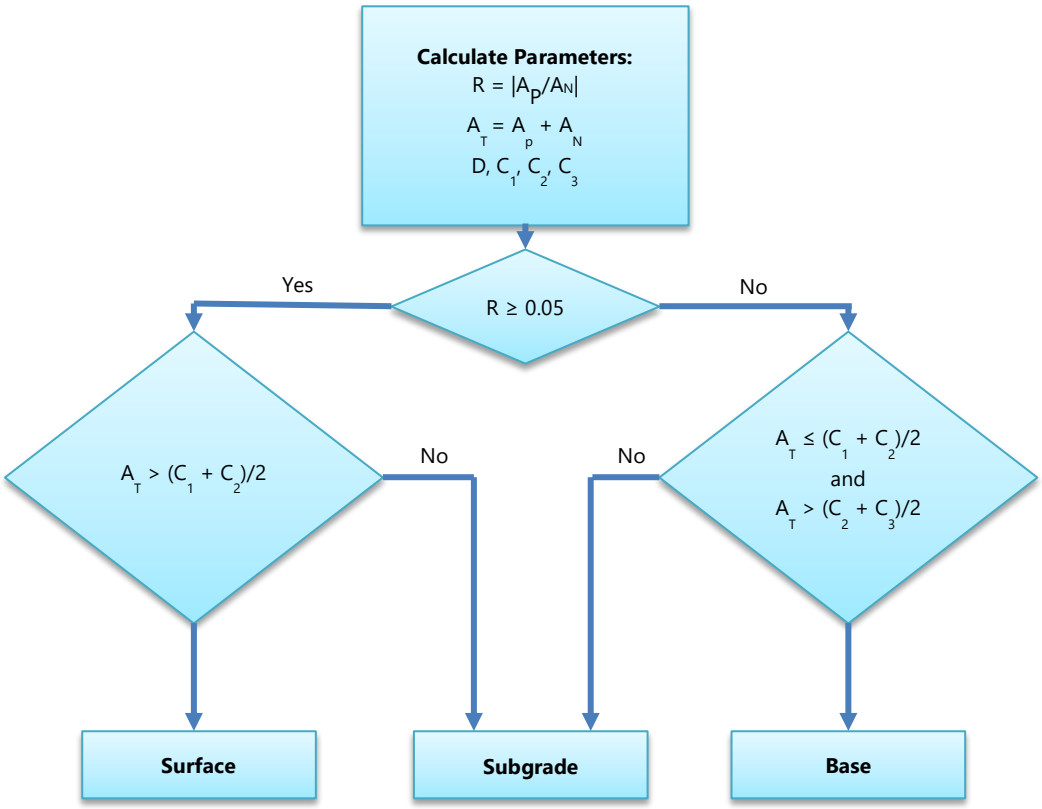

D= Maximum rut depth
A_p= Positive area (area above pavement surface line of a transverse profile)
A_n= Negative area (area below pavement surface line of a transverse profile)
C_1= (-858.21) D + 667.58, theoretical total area for HMA failure
C_2= (-1509) D -287.78, theoretical average total for base/subbase failure
C_3= (-2120.1) D – 407.95, theoretical average for subgrade failure

Figure 20. Failure layer determination using methodology by White et al. (2002)

Based on the analysis conducted for each of the transverse profiles of the test section, the lowest layer contributing to rutting was calculated for each date of collection at multiple locations along the section. Table 7 summarizes the average daily temperature at the time the transverse profile was collected and the number of locations (or transverse profiles) along the test section where the layer most contributing to rutting was surface, base, and subgrade, respectively.

As depicted in Table 7, prior to the overlay in 2001, the layer most contributing to rutting varied with the mean daily average air temperature. Contrary to what was expected, however, the AC surface layer is shown for all profiles as the layer most contributing to rutting when the air temperature is at its lowest. It is estimated from Figure 6 that the modulus of the AC layer was approximately 2,000 ksi, which represents a very stiff layer unlikely to be prone to permanent deformations. The same thing happens on the test date with the next lowest temperature (51.1°F), where 10 profiles show the AC surface layer as being the layer most contributing to rutting – the estimated AC modulus for this temperature from Figure 6 is 1,300 ksi, which is still a very stiff layer.

Table 7. Lowest layer contributing to rutting

Date	Mean daily air temperature (from MERRA) during testing (deg F)	Number of locations where rutting was related to the surface layer	Number of locations where rutting was related to the base layer	Number of locations where rutting was related to the subgrade layer
10/14/1990	71.1	6	3	2
03/12/1992	51.1	10	-	-
02/18/1993	40.8	11	-	-
02/20/1995	62.4	9	2	-
07/01/1997	80.4	-	5	6
05/11/1999	77.4	7	4	-
01/26/2001	60.1	11	-	-
03/05/2002	46.8	2	6	3
02/16/2003	44.4	9	1	-
08/05/2003	84.9	3	6	2
01/25/2006	55.8	3	4	4
08/13/2009	85.6	2	6	3
10/06/2010	66.2	3	5	3
11/20/2013	63.7	1	7	3
07/16/2015	84.2	2	7	2
01/30/2017	54.7	1	7	3

SUMMARY OF FINDINGS

LTPP test section 48_1096 is located on U.S. 90, westbound, in Medina County, Texas. U.S. 90 is a rural principal arterial with two lanes in the direction of traffic. The test section was constructed in November 1981 and incorporated into the LTPP program in January 1987 as part of the GPS 1 Asphalt Concrete (AC) on Granular Base experiment. The pavement structure at the time of its incorporation into LTPP program consisted of, from top to bottom, 7.1 inches of hot mixed, dense graded Asphalt Concrete (AC) (over three layers), a fog seal (0 inches), 8.1 inches of unbound granular base, 6 inches of bound lime-treated base, and the subgrade (fat clay with sand). The next construction event occurred in 1996 when a 0.3-inch aggregate seal coat (chip seal) was applied to the test section. On May 30, 2001, the test section received an additional 0.3-inch aggregate seal coat (chip seal). Two weeks later (June 15, 2001), the test section received a 2-inch AC overlay and became a part of the GPS 6B AC Overlay with Conventional Asphalt Cement on AC Pavement, No Milling experiment. These two construction events were combined and considered collectively as CN=3.

The memorandum was focused on the following:

1. **Examining the rapid rise in wheel path/fatigue related cracking after the 2001 overlay**. The increase observed in wheel path cracking following the AC overlay may be the result of increased traffic in the early to mid-2000s and precipitation. Additionally, the increase in cracking observed between 2006 and 2017 may be the result of aging (and more appropriately oxidizing) of the AC surface layer, leading to a more brittle material prone to fatigue cracking.
2. **Providing a history of crack sealing performed on the test section to update the contents of the LTPP database**. While only three construction events are called out in the LTPP pavement history dataset, pictures of the test section over time and the amount of sealed cracking reported in the manual distress surveys indicate crack sealing was applied to the section prior to the March 1995, November 2013, and January 2017 distress surveys. While the application of crack sealing during these periods does not have affect the pavement structure of the section, these maintenance events can affect the performance of the pavement and hence it is important to record sealed cracks. A spike in NWP longitudinal cracking, WP longitudinal cracking, and transverse cracking was observed in 1995 despite relatively low levels of cracking observed in the previous survey in 1993. The crack sealing applied during this time likely included areas of pavement that did not have cracking and therefore, cracking was over-reported in 1995.
3. **Performing a comparison between pavement design models predictions and observed pavement performance.** The AASHTO 1972 Interim Guide modified flexible pavement empirical design equation was used to assess the pavement performance using lab, field, and corrected field data. Based on the reported average moduli for each layer using lab data, W_{18} was calculated to be 94.5 million, 311.6 million using backcalculated moduli from field data, and 17.2 million using corrected field data. The corrected field data resulted in the lowest W_{18}, followed by the lab-derived W_{18}, and the field-derived W_{18}. This is mostly due to differences in the subgrade moduli used to calculate the soil support factor. Given the truck traffic observed at the test section, it appears that the pavement structure was over-designed or, more likely, that the anticipated traffic was over-estimated.

FORENSIC EVALUATION RECOMMENDATIONS

Based on the information gathered and analyzed in the above sections, the following follow-up actions are recommended:

1. LTPP close-out monitoring (FWD testing is optional but desirable).
2. Within test section coring to confirm the layer thicknesses match those reported when the test section was incorporated into the LTPP program.
3. Pursuit of additional information on the crack sealing observed on this section, particularly in 1995 and in 2017, to better understand why this section received such large quantities of crack sealing.
4. Pursuit of a more in-depth investigation of the pavement layers contributing to the observed rutting in accordance with the methodology developed under NCHRP Project 01-34a.

ADDENDUM TO MEMORANDUM: FOLLOW-UP STUDY

The desktop study analyzed available field data to explain the performance of Texas Section 48_1096. Recommendations for future field work were made as additional data gave a better insight into the performance of the section.

In cooperation with TxDOT and the LTPP Data Collection Contractor (DCC), the follow-up investigations listed below were performed:

- A manual distress and profile surveys were conducted on April 8, 2021 in accordance with LTPP protocols.
- 14 cores were obtained on April 8, 2021 from within the test section to verify layer thickness and assess the condition of pavement materials.
- Layer moduli backcalculation was performed on all FWD data collected from the section between 1990 and 2017.

These investigations are detailed next.

Manual Distress and Profile Survey Results

The LTPP Data Collection Contractor (DCC) noted upon arriving to the test section that a surface seal coat had been applied to the test section, which was not reported to the DCC. An image of the site in 2017 and Google Streetview imagery from 2018 are shown in Figure 21. According to the LTPP Directive GO-67, the application of the seal coat meant the section would have to be removed from study. While the data collected will not be entered into the LTPP database, the DCC continued with the scheduled performance monitoring in support of this investigation. Follow-up discussion with TxDOT revealed a seal coat was applied to the section in 2017. TxDOT also shared that crack-sealing occurred on test section 48_1096 in 2013, 2014, 2017, and 2021. This helps explain the increase in the amount of sealed cracking observed during the manual distress surveys conducted after 2012.

January 30, 2017 **November 2018**

Figure 21. Picture of section before (left, 2017) and after (right, 2018) seal coat application.

The distress data collected as part of the April 8, 2021 site visit is summarized in Table 8. The recent seal coat covered a lot of the existing distresses, though some of the cracking was visible in the seal coat and recorded. Therefore, the reductions in cracking between 2017 and 2021 were not unexpected. The IRI increased at a rate of 8.9 in/mile per year between 2016 and 2021, as shown in Figure 22. Given the consistent increase in the IRI values between 2006 and 2015, it is projected that the IRI will reach approximately 134 in/mile in 2021.

Table 8. Summary of current conditions

Pavement Condition Metric	Condition After AC Overlay	Previous Condition-January 2017	Latest Condition-April 2021
Transverse Crack Count	0	60	19
Transverse Crack Length	0 ft	238.5 ft	71.8 ft
Alligator Cracking	0 ft^2	335.7 ft^2	162.5 ft^2
Longitudinal Cracking Wheel Path	0 ft	3.9 ft	0 ft
Longitudinal Cracking NWP	0 ft	74.8 ft	0 ft
IRI	65.9 in/mile	94.7 in/mile (2016)	139.3 in/mile

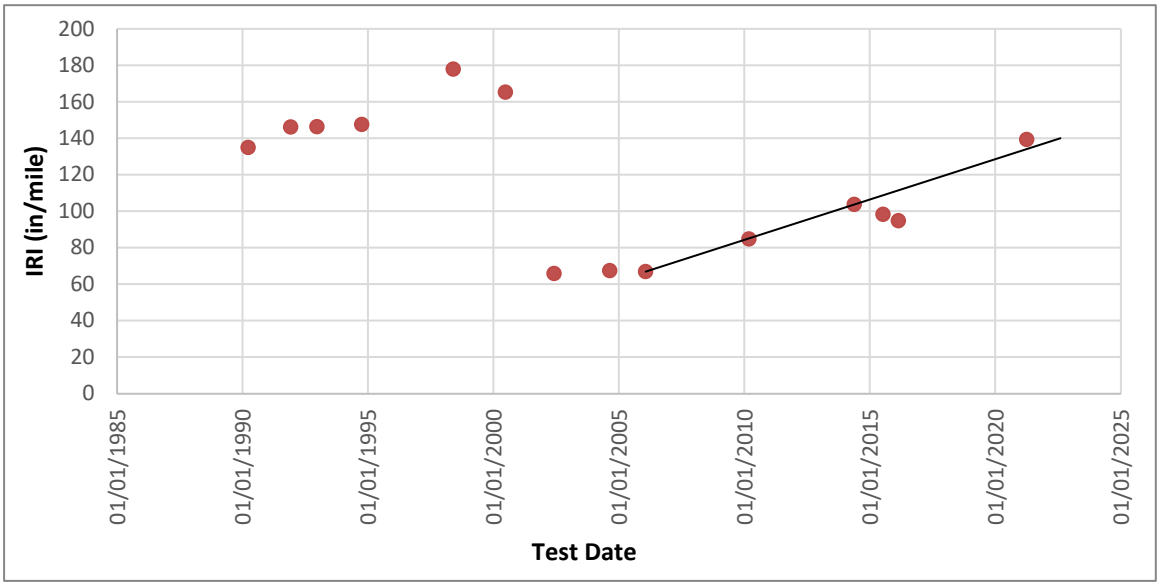

Figure 22. IRI values over time.

The appearance of cracking within the 2001 AC overlay is counterintuitive considering the analyses conducted as part of the desktop study showed the pavement to be overdesigned. The lack of surface cracking prior to the overlay would also suggest this cracking did not reflect up into the overlay. It is hypothesized that the observed cracking is related to the binder grade used in the overlay. The PG-grade of the 2001 overlay AC was a PG 70-22 binder that was unlikely to be modified as the difference between the high and low grades of the binder was less than 94, a threshold that is surpassed only by modified binders. LTPPBind was used to determine which binder grade would be recommended. The results, depicted in Figure 23, show a PG 70-10 would provide sufficient resistance to the environment and traffic, so the PG 70-22 binder used would be expected to hold up well to the climate and anticipated traffic loadings.

Performance Grade

AASHTO M323-13 Performance-Graded Asphalt Binder		
PG Temperature	High	Low
Performance Grade Temperature at 50% Reliability	65.1	-0.1
Performance Grade Temperature at 98% Reliability	65.6	-5.6
Adjustment for Traffic (AASHTO M323-13)	5.8	
Adjustment for Depth	-7.3	3.1
Adjusted Performance Grade Temperature	64.1	-2.5
Selected PG Grade	**70**	**-10**
PG Grade	**M323, PG 70-10**	

AASHTO M 332-14 Performance-Grade Asphalt Binder using Multiple Stress Creep Recovery (MSCR) Test		
PG Temperature	High	Low
Performance Grade Temperature at 50% Reliability	65.1	-0.1
Performance Grade Temperature at 98% Reliability	65.6	-5.6
Designation for traffic loading	S	
Selected PG Grade	**70**	**-10**
PG Grade	**M332, PG 70S-10**	

Temperature Report	
Lowest Yearly Air Temperature, °C:	-5.37
Low Air Temp Standard Deviation, °C:	2.23
Yearly Degree-Days > 10 Deg. °C:	4211.05
High Air Temperature of high 7 days:	39.63
Standard Dev. of the high 7 days:	1.47
Low Pavement Temperature 50%:	-5.60
Low Pavement Temperature 98%:	-11.00
High Avg Pavement Temperature of 7 Days 50%:	63.36
High Avg Pavement Temperature of 7 Days 98%:	67.24

Figure 23. Output of LTPPBind for PG-grade recommendation for AC overlay on test section 48_1096.

Coring Results

Fourteen cores were obtained from within test section 48_1096 on April 8, 2021 and are summarized in Table 9. LTPP protocols state that cores shall be taken from the material sampling areas before and after the monitoring section. However, because this was scheduled to be the close out testing, coring could be conducted from within the test section. The cores show the relative uniformity of layers 10 through 6, which do not exhibit a large variation in thickness. Layer 5 does show two areas that are thicker: (1) in the mid-lane at station 100 and (2) nearly the entire width across at station 400. The variations in thickness of layer 5 are primarily responsible for the variations in total pavement thickness between the cores.

Core photos are shown in Appendix A. The cores are all in good condition with no signs of material degradation such as cracking or stripping. The bond between the different lifts of AC appears to be strong for all cores.

Table 9. Summary of cores obtained from within section on April 8, 2021.

Core Number	Station (ft)	Offset from Fogline (ft)	Layer Thickness (in)						Total AC Thickness (in)
			L10-AC Overlay	L9-Seal Coat	L8-Seal Coat	L7-AC Surface	L6-AC Binder	L5-AC Binder	
CA01	0	6.6	2.0	0.3	0.3	1.3	0.9	5.1	9.5
CA02	100	1.6	2.0	0.4	0.3	1.0	1.0	5.1	10.0
CA03	100	3.3	2.0	0.4	0.3	1.0	1.0	5.1	10.0
CA04	100	6.6	2.0	0.4	0.3	1.0	1.0	5.4	10.3
CA05	100	9.8	2.0	0.4	0.3	1.0	1.1	5.1	9.9
CA06	100	11.5	2.0	0.4	0.3	1.0	1.0	5.1	9.8
CA07	200	6.6	2.0	0.4	0.3	1.1	1.1	5.1	10.0
CA08	300	6.6	2.0	0.4	0.3	1.0	1.1	5.1	9.9
CA09	400	1.6	2.0	0.4	0.3	1.0	1.1	5.1	9.9
CA10	400	3.3	2.0	0.4	0.3	1.0	1.0	5.3	10.1
CA11	400	6.6	2.0	0.3	0.3	1.0	1.1	5.6	10.5
CA12	400	9.8	2.0	0.3	0.3	1.0	1.1	5.6	10.5
CA13	400	11.5	2.0	0.3	0.3	1.0	1.0	5.6	10.4
CA14	500	6.6	2.0	0.3	0.3	0.9	0.9	5.0	9.5

Layer Moduli Backcalculation Results

FWD data for test section 48_1096 were downloaded from InfoPave™. The maximum deflections were temperature-adjusted using Figure 5.6 of the AASHTO 1993 Guide and normalized to a 9,000 pound load. The results (Figure 24) showed that the deflections increased between 1990 and 2000 and the deflections in the outer wheel path (OWP) were on average 18% higher compared to the mid-lane deflections. This would indicate the pavement structure is stiffer in the mid-lane compared to the OWP.

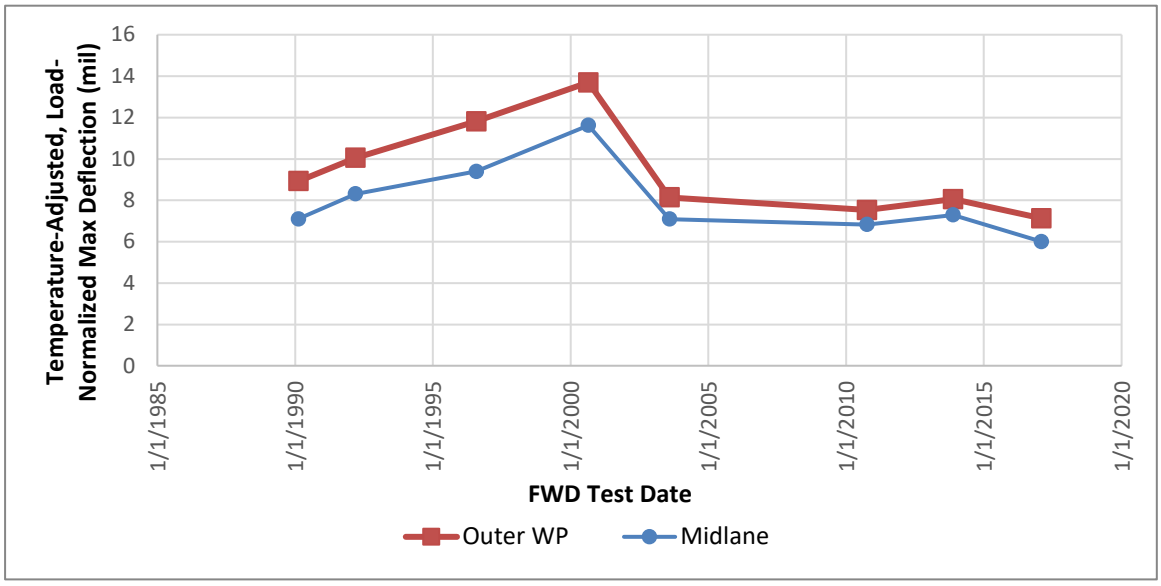

Figure 24. Maximum deflections from OWP and Mid-lane on test section 48_1096.

The subgrade modulus values for both the OWP and mid-lane were also calculated, as depicted in Figure 25. The results show the subgrade modulus dropped between 1990 and 2000 and then increased and stabilized after placement of the 2001 overlay. Additionally, the data also showed that the subgrade modulus in the OWP was on average 7% lower compared to the midline subgrade moduli values.

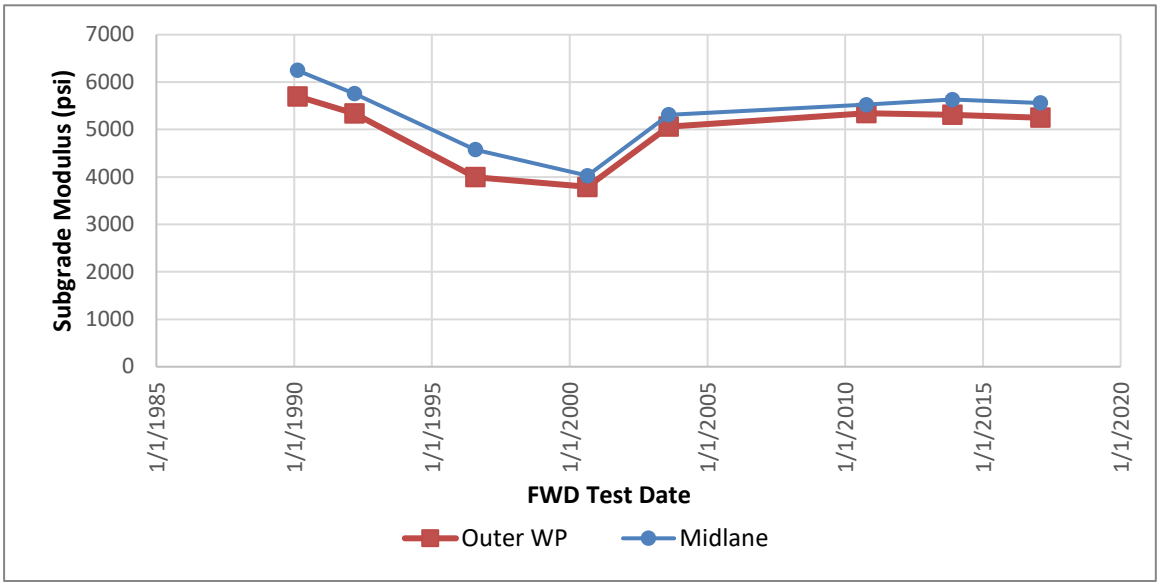

Figure 25. Average subgrade modulus from OWP and Mid-lane on test section 48_1096.

Backcalculations, using Washington Department of Transportation's EVERCALC© software, were conducted on the FWD data collected on test section 48_1096. This analysis used a different method than the one used for backcalculated moduli values available on InfoPave™ and was conducted to analyze all the FWD data in a consistent manner. The moduli values of the AC layer were calculated and temperature-adjusted using the measured mid-depth temperature of the AC during FWD testing; the results are plotted in Figure 26. Also shown are the number of occurrences where the observed rutting was related to the AC layer using the data presented in Table 7 of the desktop study. The results show that pre-overlay, there is a negative correlation between the AC modulus and the number of times the AC layer was the cause of the rutting. After the placement of the overlay, the rutting appears to come from layers other than the AC despite the AC layer modulus slowly dropping over time and then increasing in 2017. Please note that rutting data from 2021 monitoring visit will not be available due to the section going out of study.

Figure 27 shows the average AC layer coefficient as calculated using the backcalculated moduli values and the AASHTO 1993 Guide to convert modulus to a layer coefficient. The layer coefficients were limited to a maximum value of 0.6 to prevent excessively high values. The results show the AC layer coefficient was very high prior to the AC overlay in 2001. In 2011, the AC layer coefficients began to drop and reached lower values in 2013 before jumping up in 2017. The results show the decreasing layer coefficient was lagging behind the development of fatigue cracking.

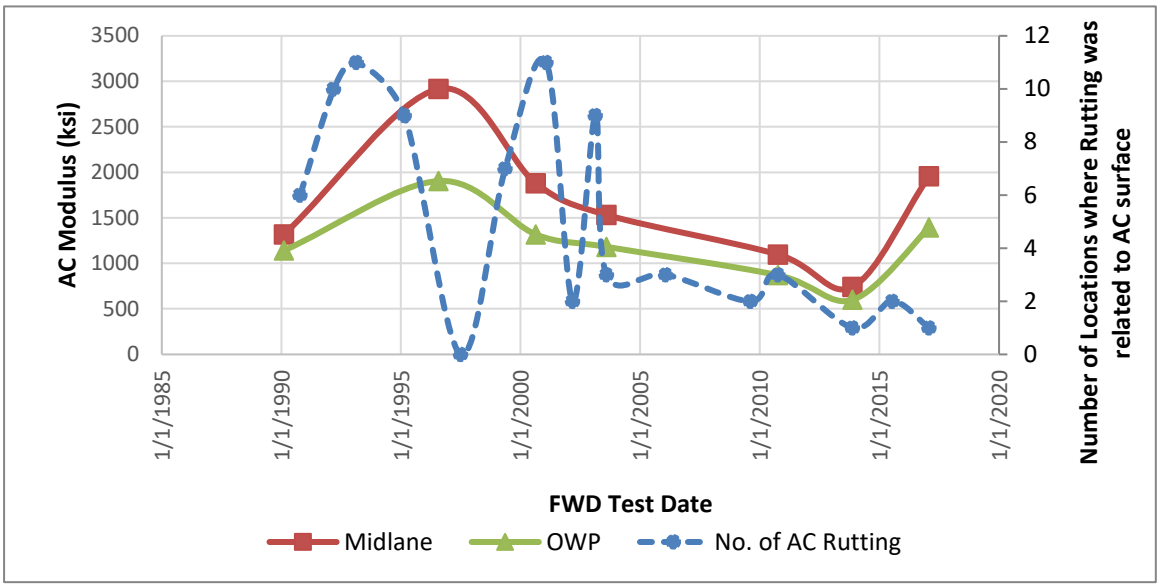

Figure 26. Average AC modulus for OWP and mid-lane, and number of locations where rutting was related to the AC surface layer.

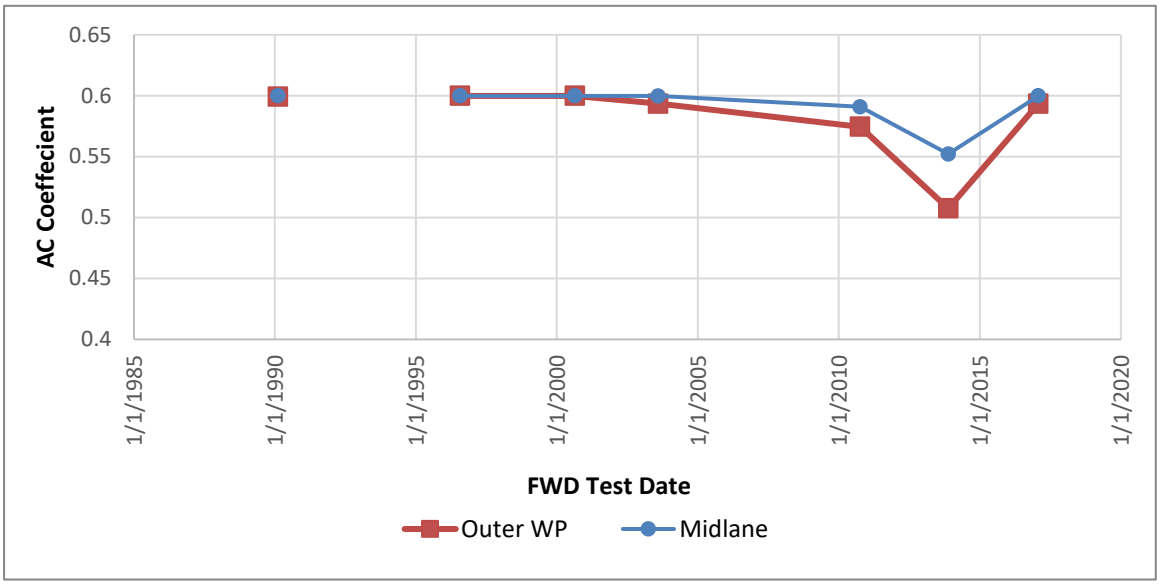

Figure 27. Average AC layer coefficient.

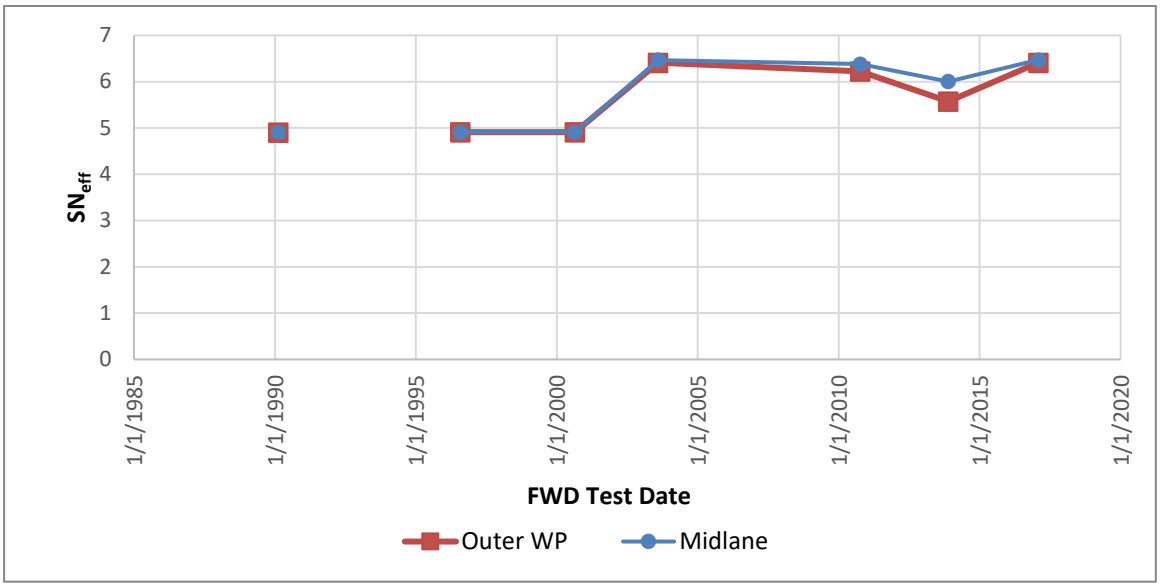

Figure 28. Average effective structural number.

Figure 28 shows the calculated effective structural number of the pavement as determined from the backcalculated moduli values. The results show the effective structural number remained relatively stable pre-overlay and then hovered around 6 after placement of the overlay. The structural number after placement of the AC overlay was higher than before the overlay, and as stated in the desktop study the original pavement appeared to be over-designed. Placement of the overlay has only increased the structural capacity, which would mean the cracking observed on the pavement surface is likely not full-depth structural cracking, but instead top-down cracking caused by a combination of AC oxidation, poor bonding between the overlay and the original AC surface, and the stresses resulting from tire-pavement interactions such as vehicle braking and accelerating.

SUMMARY OF FINDINGS

The desktop study discussed the three focus areas of this evaluation for test section 48_1096, which are below. With the additional work conducted as part of this addendum, the findings from the desktop study were revisited and updated.

1. **Examining the rapid rise in wheel path/fatigue related cracking after the 2001 overlay**. The desktop study noted several factors (increased traffic and precipitation, oxidation of AC layer) that could be responsible for the increase in wheel path cracking following the AC overlay. The temperature-adjusted AC moduli showed the layer was softening over time since the placement of the overlay which contradicts the results of the rutting analysis which showed less and less rutting being attributed to the AC layer over time. This could indicate the AC layer is stiffening. Given the desktop study suggested the pavement was over-designed for the truck traffic observed at the test section, and the additional 2-inch overlay only increased the structural number of the section, it is likely the cracking observed is related to a combination of AC oxidation, poor bonding between the overlay and the original AC surface, and the stresses resulting from tire-pavement interactions such as vehicle braking and accelerating.
2. **Providing a history of crack sealing performed on the test section to update the contents of the LTPP database**. The desktop study showed that while only three construction events were called out in the LTPP pavement history dataset, pictures of the test section over time and the

amount of sealed cracking reported in the manual distress surveys, indicated crack sealing was applied to the section prior to the March 1995, November 2013, and January 2017 distress surveys. Discussions with TxDOT confirmed that crack sealing was performed on the test section in 2013, 2014, 2017, and 2021. Records were not available to determine if crack sealing was performed on the section between 1993 and 1995, so the spike in NWP longitudinal cracking, WP longitudinal cracking, and transverse cracking observed in 1995 could be caused by aggressive crack sealing of pavement that did not have cracking. However, there was no information available to confirm this.

3. **Performing a comparison between pavement design models predictions and observed pavement performance.** The desktop study used the AASHTO 1972 Interim Guide modified flexible pavement empirical design equation to assess the pavement performance using lab, field, and corrected field data. The results showed the that given the truck traffic observed at the test section, it appeared that the pavement structure was over-designed or, more likely, that the anticipated traffic was over-estimated during the design process of the 2001 AC overlay. This would indicate the pavement had enough structural capacity to resist the development of structural cracks. Backcalculated moduli values for the AC layer showed the structural number of the pavement increased after placement of the AC overlay in 2001, which was expected. This demonstrates that the surface cracking observed in the overlay is unlikely to be structural cracks and is more likely to be top-down rather than bottom-up.

Based on the information gathered and analyzed in the follow-up investigation and given the test section is now considered Out of Study (OOS), no further activities were recommended.

Appendix A. Core Photos


C01-
CA01
48
1096
C01
CA01
N/A
3
8-Apr-21
3


C02-
CA02
48
1096
C02
CA02
N/A
3
8-Apr-21
3


C03-
CA03
48
1096
C03
CA03
N/A
3
8-Apr-21
3


C04-
CA04
48
1096
C04
CA04
N/A
3
3


C05-
CA05
48
1096
C05
CA05
N/A
3
8-Apr-21
3


C06-
CA06
48
1096
C06
CA06
N/A
3
8-Apr-21
3


C07-
CA07
48
1096
C07
CA07
N/A
3
8-Apr-21
3


C08-
CA08
48
1096
C08
CA08
N/A
3
8-Apr-21
3


C09-
CA09
48
1096
C09
CA09
N/A
3
8-Apr-21
3


C10-
CA10
48
1096
C10
CA10
N/A
3
8-Apr-21
3


C11-
CA11
48
1096
C11
CA11
N/A
3
6-Apr-21
3

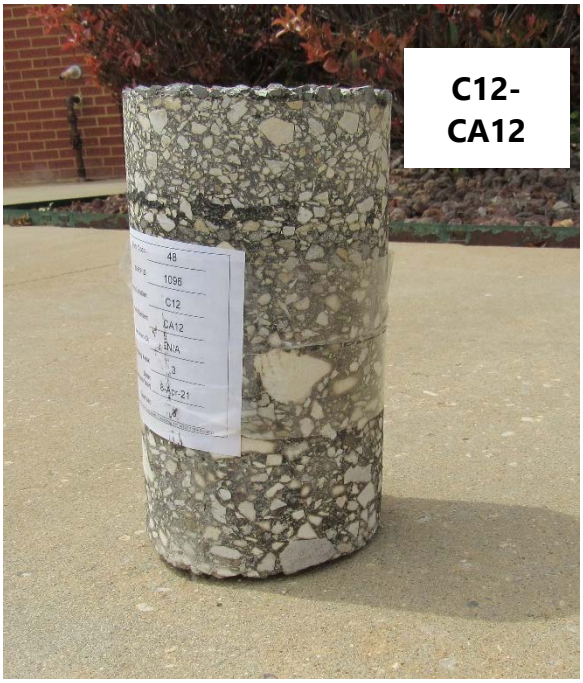
C12-
CA12
48
1096
C12
CA12
N/A
3
6-Apr-21


C13-
CA13
State Code: 48
SHRP ID: 1096
Sample Location: C13
Sample Number: CA13
Specimen ID: N/A
Sampling Area: 3
Date: (Day/Month/Year) 8-Apr-21
Field Set: 3


C14-
CA14
48
1096
C14
CA14
N/A
3
8-Apr-21
3